Published in final edited form as:
Exp Brain Res. 2010 May ; 202(3): 725–731. doi:10.1007/s00221-010-2163-0.

Neuroanatomical identification of crossmodal auditory inputs to interneurons in somatosensory cortex

Leslie P. Keniston, **Scott C. Henderson**, and **M. Alex Meredith**
Department of Anatomy and Neurobiology, Virginia Commonwealth University School of Medicine, Richmond, VA 23298, USA

Abstract

Multisensory convergence is the first, requisite step in the process that generates neural responses to events involving more than one sensory modality. Although anatomical studies have documented the merging of afferents from different sensory modalities within a given area, they do not provide insight into the architecture of connectivity at the neuronal level that underlies multisensory processing. In fact, few anatomical studies of multisensory convergence at the neuronal level have been conducted. The present study used a combination of tract-tracing, immunocytochemistry, and confocal microscopic techniques to examine the connections related to crossmodal auditory cortical inputs to somatosensory area SIV. Axons labeled from auditory cortex were found in contact with immunolabeled interneurons in SIV, some of which also colocalized vesicular glutamate transporter 1, indicating the presence of an active, glutamatergic synapse. No specific subtype of inhibitory interneuron appeared to be targeted by the cross-modal contacts. These results provide insight into the structural basis for multisensory processing at the neuronal level and offer anatomical evidence for the direct involvement of inhibitory interneurons in multisensory processing.

Keywords

Multisensory; Auditory; Tactile; Synapse; Confocal microscopy

Introduction

For separate physical events transduced by different sensory receptors (e.g., retina, cochlea, skin, etc.) to influence one another in the brain, information from the different sensory modalities must converge onto individual neurons. In this way, post-synaptic currents generated by different sensory inputs can merge on the same membrane to produce an integrated response. Therefore, convergence at the neuronal level represents the defining, first step in multisensory processing. Curiously, despite numerous anatomical studies of multisensory afferents to specific brain areas (some examples in cat include: Reinoso-Suarez and Roda 1985; Bowman and Olson 1988; Harting et al. 1992; Dehner et al. 2004; Clemo et al. 2008; Hall and Lomber 2008), almost nothing is known about convergence onto *individual neurons.*

In perhaps the only electron microscopic documentation of multisensory convergence, a bouton from a trigeminal neuron was shown to synapse with a dendrite in the cochlear nucleus (Shore et al. 2000), which was consistent with the excitatory, somatosensory–auditory responses

lkenisto@vcu.edu .
mameredi@hsc.vcu.edu

observed there (Shore et al. 2003). However, a major impediment to anatomical studies of multisensory convergence has been in discriminating and identifying recipient neurons from the neuropil. A possible solution would be to selectively label specific subpopulations of neurons. Because inhibitory interneurons represent only a fraction (~20%) of the neocortical neuronal population, immunocytochemical techniques can readily isolate their neuronal profiles (for review, see DeFelipe 1993). Therefore, a combination of immunocytochemical and tract-tracing techniques could be used to examine multisensory convergence at the neuronal level using confocal microscopy (after Vinkenoog et al. 2005). For the present study, the crossmodal projection between the auditory field of the anterior ectosylvian sulcus (FAES; Clarey and Irvine 1986; Meredith and Clemo 1989) and somatosensory area SIV (Clemo and Stein 1983) served as our model. Because the auditory FAES projection to somatosensory SIV originated from pyramidal neurons, and electrical activation of this projection suppressed somatosensory responses in SIV via GABA-ergic mechanisms (Dehner et al. 2004), it was our hypothesis that some portion of the FAES projection to SIV (see Fig. 1a) would terminate on inhibitory interneurons. A preliminary abstract of these results has been reported (Keniston et al. 2006).

Methods

All procedures were conducted in accord with the National Research Council's Guidelines for the Care and Use of Mammals in Neuroscience and Behavioral Research (2003) and with the approval of the Animal Care and Use Committee of the Virginia Commonwealth University. The following procedures and assumptions are essentially the same as Vinkenoog et al. (2005) for confocal identification of anatomical contacts onto immunocytochemically identified neurons.

Surgery, tracer injection, and histological processing

Cats (n = 3) were prepared as described in detail (Dehner et al. 2004) except that the neuroanatomical tracer F-BDA (Fluoroemerald; #D1820, Molecular Probes; 10% in 0.1 M phosphate buffer) was used. To inject the FAES, a 5-μl syringe with the tracer was held by a carrier angled 53-60E (from vertical), with 35-40E cant (posterior from coronal plane) and the needle tip was inserted at a point 0.8–1.5 mm anterior to the vertical limb of the AES to a depth of 5.25–5.70 mm (after Dehner et al. 2004). The tracer was pressure-injected into the auditory FAES. Following a 7- to 9-day period for tracer transport, the animal was euthanized, fixed, and the brain removed for processing. The cortex surrounding the anterior ectosylvian sulcus was stereotaxically blocked, cryoprotected, and sectioned (50 μm) serially in the coronal plane on a freezing microtome. A series of sections taken at 200-μm intervals was processed for BDA using an avidin–biotin reaction (Veenman et al. 1992) with nickel–cobalt (Ni–Co) intensification. This series was used to confirm, using light microscopy, the location of the FAES injection site, which was required to label the medial and dorsomedial portions of the bank of the AES where the FAES lies submerged in the middle ectosylvian gyrus (FAES criteria of Dehner et al. 2004). Light microscopy was also used to select, by the presence of labeled axons, the areas of SIV (defined as the anterior-dorsal bank of the AES; criteria of Clemo and Stein 1983) to be examined subsequently with confocal laser scanning microscopy.

Immunocytochemistry

To visualize inhibitory interneurons, tissue sections containing somatosensory area SIV were immunolabeled for the presence of Calbindin (CB), Calretinin (CR), or Parvalbumin (PV)-positive interneurons (calcium-binding proteins that co-localize with GABA; e.g., Clemo et al. 2003). Serial coronal sections were taken for each marker at 200-μm intervals through SIV. First, the sections were washed (3 × 5 min) in phosphate-buffered 0.9% saline (PBS). Nonspecific blocking was done in 10% normal goat serum (NGS)/1% bovine serum albumin

(BSA) in PBS (1 h at RT). Primary antibodies used were either polyclonal rabbit anti-feline parvalbumin (courtesy of CW Heizmann; see Stichel et al. 1986), mouse monoclonal anti-calbindin, (C-9848, Sigma), or mouse monoclonal anti-calretinin (MAB1568, Chemicon) at 1:750 dilution ratio in 1% NGS/1% BSA in phosphate buffered saline (PBS). Primary antibody incubation was accompanied by gentle agitation for 1 h at room temperature, followed by a minimum of 12 h at 4°C. Following primary incubation, each series was washed in PBS (3 × 5 min). Next, to enhance F-BDA tracer visualization, sections were incubated in Streptavidin–Fluorescein (FITC) at 1:100 in PBS with gentle agitation (1 h at RT). Finally, each series was exposed to a secondary antibody of goat anti-mouse IgG conjugated to either Rhodamine (TRITC) and/or Cy5 at 1:100 with mild agitation (1 h at RT). Each series was wet mounted (Biomedia Gel/Mount), cover slipped, and sealed. Procedural controls included a non-specific absorption series using a pooled Mouse IgG serum fraction at 1:750 and a deletion series with no application of primary antibody to assess secondary antibody and streptavidin specificity.

In a separate series of sections taken from one case, sections received additional immunoprocessing to visualize vesicular glutamate transporter 1 (vGlut1), a pre-synaptic membrane-bound transporter that is critical for quantal regulation and release of synaptic vesicles at active glutamatergic synapses (Fremeau et al. 2001; Graziano et al. 2008). In addition to the presence of FITC-BDA and PV immunoreactive interneurons (as described above), this series of sections was also incubated with a monoclonal antibody raised in mouse against recombinant rat vGlut1 protein (MAB5502, Chemicon) at 1:1,000 dilution. The vGlut1 primary antibody was then exposed to a secondary antibody (goat anti-mouse IgG) conjugated to fluorescent marker Cy5 at 1:100 dilution. Nonspecific controls and mounting were identical to the other series, described earlier.

Confocal laser scanning microscopy

Images were derived only from those cases in which injections were restricted to the medial part of the FAES (Clarey and Irvine 1986; Meredith and Clemo 1989) that resulted in terminal labeling in SIV (defined by Clemo and Stein 1983). Selected sections were examined by a laser scanning confocal microscope (TCS SP2 AOBS, Leica Microsystems). First, low magnification terminal fields of FAES axons in SIV were imaged to facilitate selection of optimal bouton fields where subsequent high-magnification (63× oil immersion lens; NA 1.4) image stacks were then collected. PMT voltage, gain, and offset were set at the time of capture to optimize signal to noise ratios. Confocal imaging was sampled with an average dimension of 761 × 761 × 119 pixels.

Data analysis

Post imaging stacks were imported into Volocity (Improvision, Lexington, Ma.) on a PC workstation. To correct for point-spread function distortions in the *z* axis, 3-D adaptive blind deconvolution processing was conducted (Auto-Quant, Media Cybernetics, Bethesda, Md.). For ease of examination, both native and deconvolved stacks were then cropped into individual stacks comprising one or two immunolabeled neuron(s) and its surround. The trimmed stacks were then reimported into Volocity and examined for contacts in three dimensions. A contact was defined as a FITC-labeled axonal swelling/bouton and a TRTC/Cy5 labeled neuron between which no visible gap could be observed from any point of rotation. The immunocytochemical type of each SIV neuron examined (CB, CR, and PV), the presence (or absence) of FAES contact(s), and the number of contacts and their location on the neuron (somatic, proximal dendrite) were tabulated.

Identification of vGlut1 label in correspondence with synaptic contacts involved identical confocal methods. Designation of a contact as representing an active synapse required that the 3-dimensional examination of an axon swelling show (1) no gap between it and the postsynaptic

membrane of a well-defined immunopositive neuron, and (2) the presence of vGlut1-positive patch or disk. Furthermore, (3) the vGlut1 label had to be present inside the bouton swelling near the apposition of the pre- and postsynaptic membranes (Hagiwara et al. 2005). Neuronal profiles that met all three criteria were regarded as representing an active, glutamatergic synapse between an auditory FAES axon terminal and a somatosensory SIV interneuron. The number and location (cell body or dendrite) of examined contacts with PV-immunopositive interneurons with or without vGlut1 colocalization were tabulated.

Results

Immunocytochemical procedures to visualize Calbindin (CB), Calretinin (CR) or Parvalbumin (PV) revealed morphological patterns indicative of interneurons (e.g., spherical, non-pyramidal shaped somas, multipolar or bipolar with horizontal or vertical-oriented dendrites; for review see DeFelipe 1993) that were distributed in distinctive laminar patterns within the SIV consistent with previous reports (Clemo et al. 2003). Confocal laser scanning microscopy of labeled SIV interneurons generated a total of 39 image stacks for which 3-D renderings were created. The average physical stack size was 157 × 157 × 16 μm, yielding an average voxel dimension of 269 × 269 × 246 nm. With an average bouton diameter of 0.5–1 μm, these structures were well within the resolving power of both the initial microscopy and ensuing computer modeling.

From the volume-rendered models, a total 283 immunocytochemically labeled SIV neurons were examined. They were all identified within the supragranular layers where these forms of interneurons have been previously described (Clemo et al. 2003) and where boutons of FAES axons are known to preferentially terminate (Dehner et al. 2004). Of these, 3-D rotation and analysis demonstrated that 112 (40%) received at least one anatomical contact by inputs labeled from the FAES. Examples of such crossmodal contacts are presented for each type of SIV immunolabeled neuron in Fig. 1. In each case, a FITC-labeled axon from the FAES passed in close proximity to an immunololabeled SIV neuron and exhibited one or more swellings in apposition to the surface of the SIV neuron (defined here as an anatomical contact). Three-dimensional inspection of the bouton/neuron relationship confirmed the contact between the two structures. Examples of FAES-SIV contacts were observed among each type of immunopositive (CB, CR, PV) neuron examined in SIV and the proportion of each interneuron type with FAES contacts was strikingly similar (see Table 1). In most cases (57%; 64/112), one FAES contact was identified in association with an SIV interneuron, while multiple contacts (up to 6 per neuron) were also frequently (43%; 48/112) observed. FAES contacts were found on the somas as well as dendrites of FAES interneurons. Again, similar proportions of contacts were found on the somas of the different SIV neurons (CB 60%; CR 75%; PV 72%) as well as on their dendrites (CB 55%; CR 54%; PV 34%; note that values sum >100% because some had contacts on both soma and dendrites). Thus, no class of SIV interneuron appeared to receive preferential innervation from FAES, and anatomical contacts from FAES inputs were not restricted to a particular neuronal compartment.

To correlate anatomical contact sites with features definitive of synapses, a subset of axon-interneuron contacts was examined further for the presence of the glutamate vesicular transporter, vGlut1. This molecule identifies an excitatory synapse (Takamori et al. 2000) and is a specific marker of vesicular glutamate (Herzog et al. 2006). A total of six image stacks were taken from tissue containing FITC-BDA labeled axons from auditory FAES and immunoreacted for PV-positive SIV interneurons as well as the vGlut1 molecule. For this analysis, the average physical stack size was 180 × 180 × 7 μm, giving an average voxel dimension of 92 × 92 × 364 nm. From the confocal stacks, 33 neurons identified as PV-positive also exhibited contacts (n = 59) with FAES FITC-labeled axons. A majority (54%; 32/59) of

these anatomical contacts were positive for vGlut1 immunolabeling (illustrated in Fig. 2), indicative of a functional synapse.

Discussion

The combination of anatomical techniques used here visualized the simplest form of multisensory convergence at the neuronal level: inputs from one modality (auditory, FAES) made contact with individual neurons in the representation of another modality (somatosensory, SIV). Furthermore, the presence of vGlut1 at FAES contacts with PV-positive SIV interneurons indicates that the synapse is active and glutamatergic (Takamori et al. 2000; Hagiwara et al. 2005; Herzog et al. 2006). That the vGlut1 molecule was present at the FAES-SIV synapse is also consistent with the origin of the projection from pyramidal neurons (generally regarded as glutamatergic) in FAES (Dehner et al. 2004).

The combination of anatomical techniques used here (modified from Vinkenoog et al. 2005) identified anatomical contacts with submicron resolution onto PV-, CB-, and CR-positive neurons, or identified functional synapses (using vGlut1 marker) onto PV-positive neurons. In the latter condition, approximately half of the anatomically identified contacts were demonstrated to be functional synapses. This is not surprising because other studies have observed differences between confocal and electron microscopic identification of synapses (e.g., da Costa and Martin 2009). However, if the same proportions identified for PV-positive neurons represent functional synapses on CB- and CR-positive neurons, then these data suggest that neither type of SIV inhibitory interneuron is preferentially targeted by the auditory FAES projection. This issue deserves further investigation. Also, it should be noted that these observations do not rule out the likely contact of FAES projections to aspects of SIV principal neurons, whose connectivity must be addressed using other methodologies.

The presence of excitatory inputs from auditory FAES onto SIV neurons would suggest that these contacts would underlie the generation of bimodal auditory-somatosensory neurons in this region. Numerous electrophysiological examinations of SIV have been conducted, yet bimodal neurons (e.g., those that showed suprathreshold activation to separate auditory and somatosensory stimulation) were rarely encountered (1% bimodal Clemo and Stein 1983; 0% Rauschecker and Korte 1993; 8% Jiang et al. 1994; 2% Benedek et al. 1996; 2% Dehner et al. 2004). Although several studies in this region have indicated that bimodal neurons tend to be located at the borders between adjoining representations of different sensory modalities (Meredith 2004; Wallace et al. 2004), the present tissue samples were obtained distant from this transition zone to avoid labeling-artifact from the FAES injection site. Furthermore, stimulation of the FAES projection did not reveal any SIV neurons activated by separate auditory and somatosensory stimulation (i.e., bimodal), and it seems possible that the recording properties of the electrodes may have been insensitive for sampling activity of these characteristically small neurons (Clemo et al. 2003). However, their influence was indirectly measurable on SIV principal neurons, since 70% had their somatosensory-evoked activity suppressed by the crossmodal inputs (Dehner et al. 2004). Consequently, these principal SIV neurons were neither unisensory nor bimodal but, due to the modulation of their somatosensory responses by auditory activation of inhibitory neurons, were designated as a subthreshold form of multisensory neuron. As such, they join the growing number of examples of subthreshold multisensory neurons identified in other regions of the brain (Meredith et al. 2006; Sugihara et al. 2006; Allman and Meredith 2007; Carriere et al. 2007; Clemo et al. 2007; Allman et al. 2008, 2009; Meredith and Allman 2009; Keniston et al. 2009). The present results, therefore, are consistent with the projection of auditory FAES inputs to SIV inhibitory interneurons that, in turn, subtly modulate the somatosensory activity of principle SIV neurons (summarized in Fig. 14, Dehner et al. 2004).

Ultimately, the present study provides anatomical evidence that inhibitory interneurons, of a variety of subtypes, have the potential to play a key role in cortical multisensory processing. Inhibitory interneurons are well known for their role in shaping modality-specific receptive field properties, such as sharpening of frequency tuning in auditory cortex (e.g., Fuzessery and Hall 1996; Richter et al. 1999; Wang et al. 2000), orientation tuning in visual areas (Sillito et al. 1985), and spatial inhibition in barrel field/somatosensory cortex (e.g., Chowdhury and Rasmusson 2002; Li et al. 2002). In the present study, auditory FAES inputs to SIV were distributed in comparable proportions to each of the different sub-classes of interneuron (i.e., PV-, CR- and CB-positive) suggesting that FAES inputs similarly drive interneurons with different functional and connectional patterns. In addition, individual classes of inhibitory interneurons are extensively interconnected into local networks (Amitai et al. 2002; Markram et al. 2004), such that a given interneuron can influence a much larger pool of similar neurons and, thereby, regulate large populations of cortical neurons in a synchronous fashion. Similarly, the effects of the FAES projection to SIV are likely to be distributed broadly across the different cortical layers and region and may underlie general, non-specific effects, such as attention (e.g., see Teder-Salejarvi et al. 1999), regulation of regional oscillatory patterns (Lakatos et al. 2007), and/or the dynamic control of firing modes (Wang et al. 2007).

Acknowledgments

This work was supported by NIH-NINDS Center Core Grant to VCU Anatomy and Neurobiology Microscopy Facility and NIH Grant NS39460 (to MAM).

References

Allman B, Meredith MA. Multisensory processing in ‘uni-modal’ neurons: cross-modal subthreshold auditory effects in cat extrastriate visual cortex. J Neuorphysiol 2007;98:545–549.

Allman BL, Bittencourt-Navarrete RE, Keniston LP, Medina A, Wang MY, Meredith MA. Do cross-modal projections always result in multisensory integration? Cereb Cortex 2008;18:2066–2076. [PubMed: 18203695]

Allman BL, Keniston LP, Meredith MA. Not just for bimodal neurons anymore: the contribution of unimodal neurons to cortical multisensory processing. Brain Topogr 2009;21:157–167. [PubMed: 19326204]

Amitai Y, Gibson JR, Beierlein M, Patrick SL, Ho AM, Connors BW, Golomb D. The spatial dimensions of electrically coupled networks of interneurons in the neocortex. J Neurosci 2002;22:4142–4152. [PubMed: 12019332]

Benedek G, Fischer-Szatmari L, Kovacs G, Perenyi J, Katoh YY. Visual, somatosensory and auditory modality properties along the feline suprageniculate-anterior ectosylvian sulcus/insular pathway. Prog Brain Res 1996;112:325–334. [PubMed: 8979839]

Bowman EM, Olson CR. Visual and auditory association areas of the cat's posterior ectosylvian gyrus: cortical afferents. J Comp Neurol 1988;272:30–42. [PubMed: 2454976]

Carriere BN, Royal DW, Perrault TJ, Morrison SP, Vaughan JW, Stein BE, Wallace MT. Visual deprivation alters the development of cortical multisensory integration. J Neurophysiol 2007;98:2858–2867. [PubMed: 17728386]

Chowdhury SA, Rasmusson DD. Comparison of receptive field expansion produced by GABA(B) and GABA(A) receptor antagonists in raccoon primary somatosensory cortex. Exp Brain Res 2002;144:114–121. [PubMed: 11976765]

Clarey JC, Irvine DR. Auditory response properties of neurons in the anterior ectosylvian sulcus of the cat. Brain Res 1986;386:12–19. [PubMed: 3779403]

Clemo HR, Stein BE. Organization of a fourth somatosensory area of cortex in cat. J Neurophysiol 1983;50:910–925. [PubMed: 6631469]

Clemo HR, Keniston L, Meredith MA. A comparison of the distribution of GABA-ergic neurons in cortices representing different sensory modalities. J Chem Neuroanat 2003;26:51–63. [PubMed: 12954530]

Clemo HR, Allman BL, Donlan MA, Meredith MA. Sensory and multisensory representations within the cat rostral suprasylvian cortex. J Comp Neurol 2007;503:110–127. [PubMed: 17480013]

Clemo HR, Sharma GK, Allman BL, Meredith MA. Auditory projections to extrastriate visual cortex: connectional basis for multisensory processing in 'unimodal' visual neurons. Exp Brain Res 2008;191:37–47. [PubMed: 18648784]

Da Costa NM, Martin KAC. Selective targeting of the dendrites of corticothalamic cells by thalamic afferents in area 17 of the cat. J Neurosci 2009;29:13919–13928. [PubMed: 19890002]

DeFelipe J. Neocortical neuronal diversity: chemical heterogeneity revealed by colocalization studies of classic neurotransmitters, neuropeptides, calcium-binding proteins, and cell surface molecules. Cereb Cortex 1993;3:273–289. [PubMed: 8104567]

Dehner LR, Keniston LP, Clemo HR, Meredith MA. Cross-modal circuitry between auditory and somatosensory areas of the cat anterior ectosylvian sulcal cortex: a 'new' inhibitory form of multisensory convergence. Cereb Cortex 2004;14:387–403. [PubMed: 15028643]

Fremeau RT Jr, Troyer MD, Pahner I, Nygaard GO, Tran CH, Reimer RJ, Bellocchio EE, Fortin D, Storm-Mathisen J, Edwards RH. The expression of vesicular glutamate transporters defines two classes of excitatory synapse. Neuron 2001;31:247–260. [PubMed: 11502256]

Fuzessery ZM, Hall JC. Role of GABA I shaping frequency tuning and creating FM sweep selectivity in the inferior colliculus. J Neurophysiol 1996;76:1059–1073. [PubMed: 8871220]

Graziano A, Liu XB, Murray KD, Jones EG. Vesicular glutamate transporters define two sets of glutamatergic afferents to the somatosensory thalamus and two thalamocortical projections in the mouse. J Comp Neurol 2008;507:1258–1276. [PubMed: 18181146]

Hagiwara A, Fukazawa Y, Deguchi-Tawarada M, Ohtsuka T, Shigemoto R. Differential distribution of release-related proteins in the hippocampal CA3 area as revealed by freeze-fracture replica labeling. J Comp Neurol 2005;489:195–216. [PubMed: 15983999]

Hall AJ, Lomber SG. Auditory cortex projections target the peripheral field representation of primary visual cortex. Exp Brain Res 2008;190:413–430. [PubMed: 18641978]

Harting JK, Updyke BV, Van Lieshout DP. Corticotectal projections in the cat: anterograde transport studies of twenty-five cortical areas. J Comp Neurol 1992;324:379–414. [PubMed: 1401268]

Herzog E, Takamori S, Jahn R, Brose N, Wojcik SM. Synaptic and vesicular co-localization of the glutamate transporters VGLUT1 and VGLUT2 in the mouse hippocampus. J Neurochem 2006;99:1011–1018. [PubMed: 16942593]

Jiang H, Lepore F, Ptito M, Guillemot JP. Sensory modality distribution in the anterior ectosylvian cortex (AEC) of cats. Exp Brain Res 1994;97:404–414. [PubMed: 8187853]

Keniston LP, Henderson SC, Meredith MA. Confocal identification of multisensory convergence on cortical neurons in cat. Soc Neurosci Abstr 2006;137:18.

Keniston LP, Allman BA, Meredith MA, Clemo HR. Somatosensory and multisensory properties of the medial bank of the ferret rostral suprasylvian sulcus. Exp Brain Res 2009;196:239–251. [PubMed: 19466399]

Lakatos P, Chen CM, O'Connell MN, Mills A, Schroeder CE. Neuronal oscillations and multisensory interaction in primary auditory cortex. Neuron 2007;53:279–292. [PubMed: 17224408]

Li CX, Callaway JC, Waters RS. Removal of GABAergic inhibition alters subthreshold input in neurons in forepaw barrel sub-field (FBS) in rat first somatosensory cortex (SI) after digit stimulation. Exp Brain Res 2002;145:411–428. [PubMed: 12172653]

Markram H, Toledo-Rodriguez M, Wang Y, Gupta A, Silberberg G, Wu C. Interneurons of the neurocortical inhibitory system. Nat Neurosci Rev 2004;5:793–807.

Meredith, MA. Cortico-cortical connectivity and the architecture of cross-modal circuits. In: Spence, C.; Calvert, G.; Stein, B., editors. Handbook of multisensory processes. MIT Press; 2004. p. 343-355.

Meredith MA, Allman BL. Subthreshold multisensory processing in cat auditory cortex. NeuroReport 2009;20:126–131. [PubMed: 19057421]

Meredith MA, Clemo HR. Auditory cortical projection from the anterior ectosylvian sulcus (Field AES) to the superior colliculus in the cat: an anatomical and electrophysiological study. J Comp Neurol 1989;289:687–707. [PubMed: 2592605]

Meredith MA, Keniston LR, Dehner LR, Clemo HR. Crossmodal projections from somatosensory area SIV to the auditory field of the anterior ectosylvian sulcus (FAES) in cat: further evidence for

subthreshold forms of multisensory processing. Exp Brain Res 2006;172:472–484. [PubMed: 16501962]

Rauschecker JP, Korte M. Auditory compensation for early blindness in cat cerebral cortex. J Neurosci 1993;13:4538–4548. [PubMed: 8410202]

Reinoso-Suarez F, Roda JM. Topographical organization of the cortical afferent connections to the cortex of the anterior ectosylvian sulcus in the cat. Exp Brain Res 1985;59:313–324. [PubMed: 2411583]

Richter K, Hess A, Scheich H. Functional mapping of transsynaptic effects of local manipulation of inhibition in gerbil auditory cortex. Brain Res 1999;831:184–199. [PubMed: 10411998]

Shore SE, Vass Z, Wys NL, Altschuler RA. Trigeminal ganglion innervates the auditory brainstem. J Comp Neurol 2000;419:271–285. [PubMed: 10723004]

Shore SE, El KH, Lu J. Effects of trigeminal ganglion stimulation on unit activity of ventral cochlear nucleus neurons. Neurosci 2003;119:1085–1101.

Sillito AM, Salt TE, Kemp JA. Modulatory and inhibitory processes in the visual cortex. Vision Res 1985;25:375–381. [PubMed: 2862740]

Stichel CC, Kagi U, Heizmann CW. Parvalbumin in cat brain: isolation, characterization and localization. J Neurochem 1986;47:46–53. [PubMed: 3711911]

Sugihara T, Diltz MD, Averbeck BB, Romanski LM. Integration of auditory and visual communication information in the primate ventrolateral prefrontal cortex. J Neurosci 2006;26:11138–11147. [PubMed: 17065454]

Takamori S, Rhee JS, Rosenmund C, Jahn R. Identification of a vesicular glutamate transporter that defines a glutamatergic phenotype in neurons. Nature 2000;407:189–194. [PubMed: 11001057]

Teder-Salejarvi WA, Munte TF, Sperlich F, Hillyard SA. Intra-modal and cross-modal spatial attention to auditory and visual stimuli. An event-related brain potential study. Brain Res Cogn Brain Res 1999;8:327–343. [PubMed: 10556609]

Veenman CL, Reiner A, Honig MG. Biotinylated dextran amine as an anterograde tracer for single- and double-labeling studies. J Neurosci Methods 1992;41:239–254. [PubMed: 1381034]

Vinkenoog M, van den Oever MC, Uylings HB, Wouterlood FG. Random or selective neuroanatomical connectivity. Study of the distribution of fibers over two populations of identified interneurons in cerebral cortex. Brain Res Brain Res Protoc 2005;14:67–76. [PubMed: 15721812]

Wallace MT, Ramachandran R, Stein BE. A revised view of sensory cortical parcellation. Proc Natl Acad Sci USA 2004;101:2167–2172. [PubMed: 14766982]

Wang J, Caspary D, Salvi RJ. GABA-A antagonist causes dramatic expansion of tuning in primary auditory cortex. Neuro-Report 2000;11:1137–1140.

Wang X, Wei Y, Vaingankar V, Wang Q, Koepsell K, Sommer FT, Hirsch HA. Feedforward excitation and inhibition evoke dual modes of firing in the cat's visual thalamus during naturalistic viewing. Neuron 2007;55:465–478. [PubMed: 17678858]

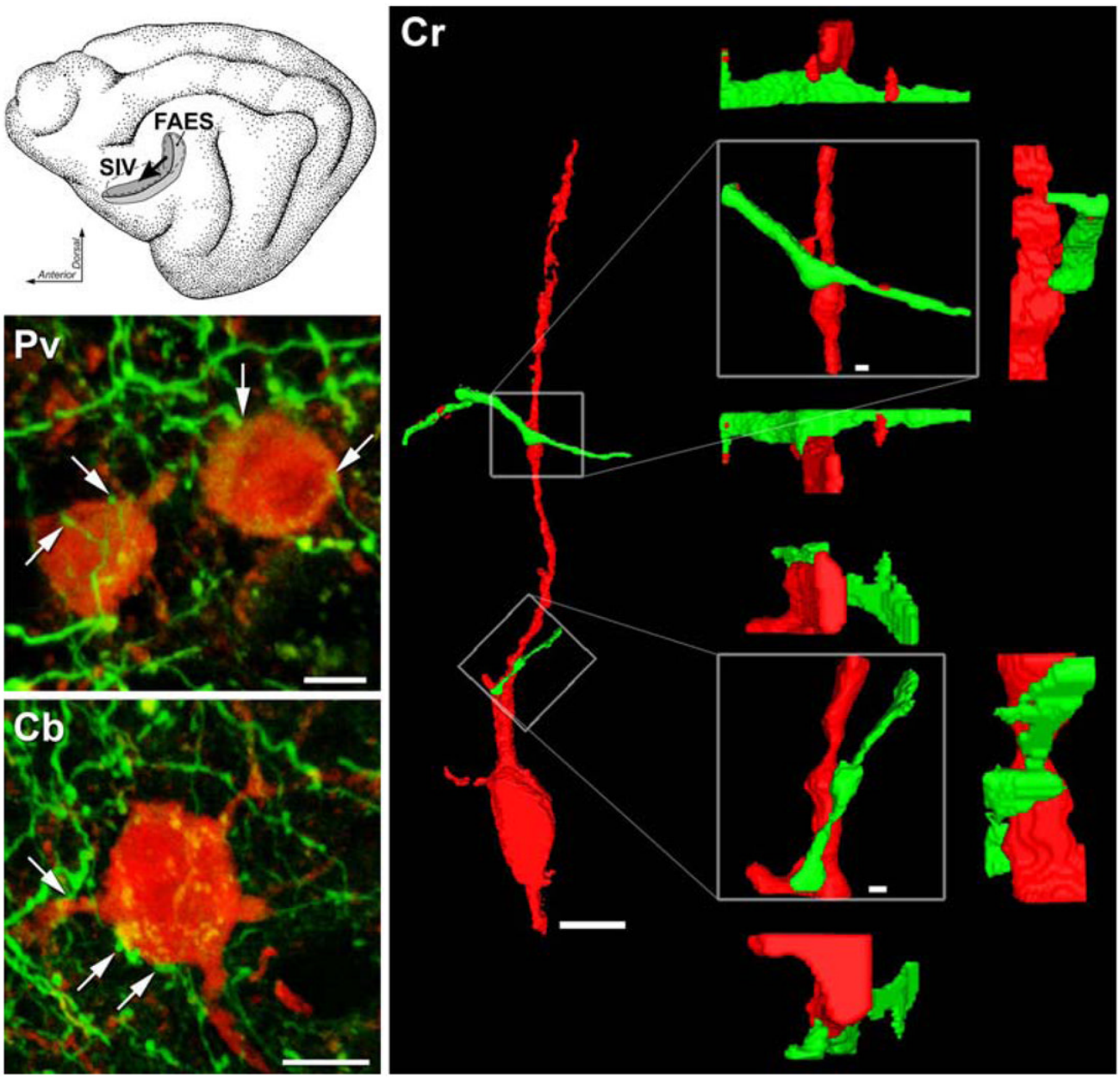

Fig. 1.

Confocal images of somatosensory SIV neurons (*red*) contacted by boutons that originated in auditory FAES (*green*). (*Top inset*) The schematic of the cat cortex shows the anterior ectosylvian sulcus (*opened*) which contains somatosensory (Area SIV) receiving inputs (*arrow*) from auditory (FAES). (Cr) A 3-dimensional rendering of a trimmed confocal stack containing Calretinin-positive SIV interneuron (*red*; note also its definitive bipolar shape, *scale bar* 10 μm) was contacted by two axons (*green*) that were labeled from auditory area FAES. Each of the axo-dendritic points of contact are enlarged on the right (*boxed*; *scale bar* 1.0 μm) to reveal the putative bouton swelling. The point of contact is rotated from this central panel (*boxed*) by 90° above, below, and to the side to demonstrate that the green-labeled synaptic swelling maintained contact with the red-labeled dendrite when viewed from each of the different perspectives. (*Pv* & *Cb*) Voxel models of two other SIV inhibitory interneurons

(Parvalbumin-*top*; Calbindin-*bottom*) made from images taken with a 63×/NA 1.4 objective lens, cropped to individual neuron(s). In each model, projections from auditory FAES terminate in close apposition (at *arrows*) with the depicted SIV interneurons, such that upon 3-D rotation of the image revealed no gaps between the two surfaces (rotations not shown). *Scale bars* 5 μm

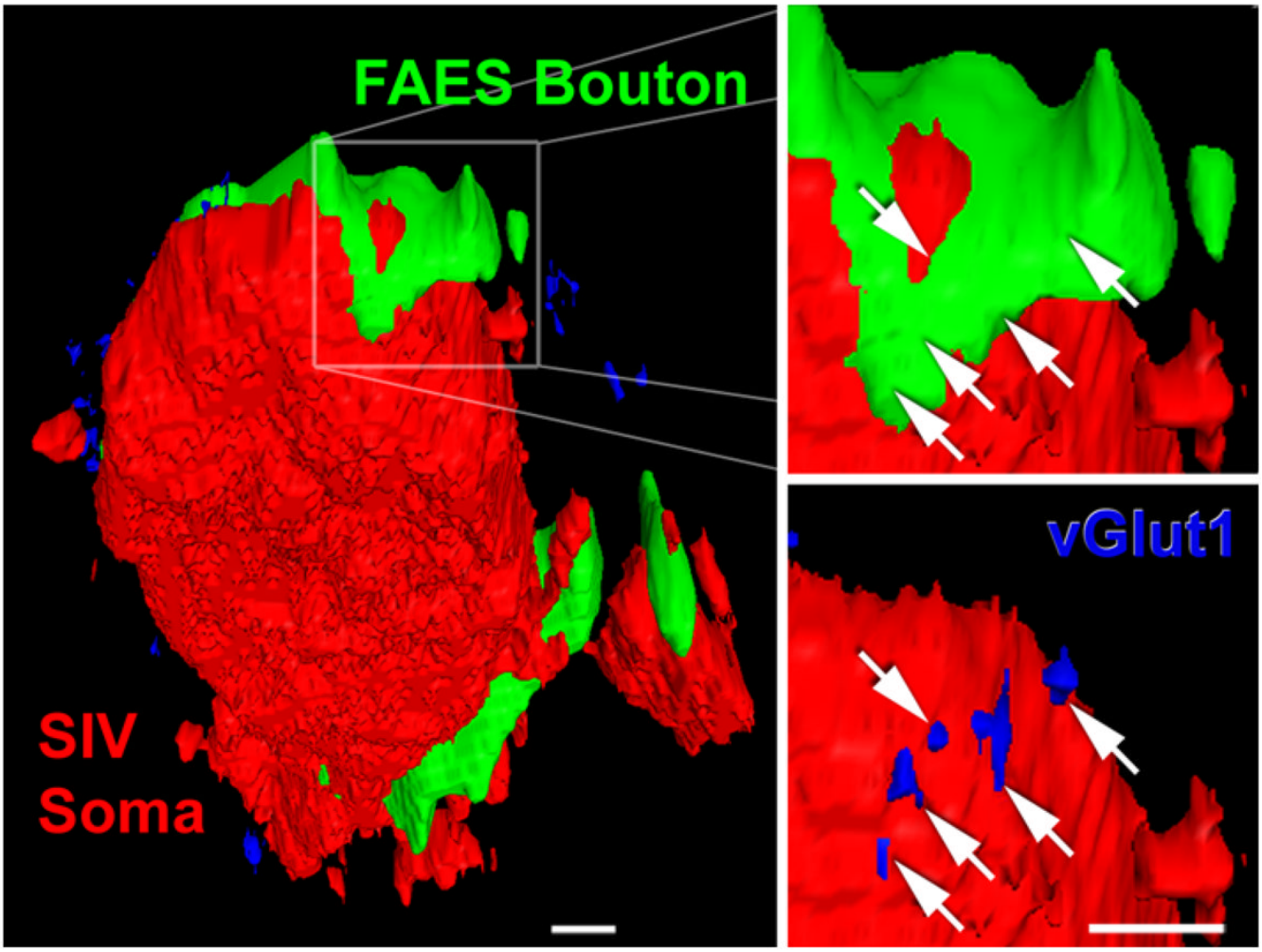

Fig. 2.

A FAES bouton in contact with SIV interneuron co-localizes vesicular glutamate transporter 1, indicative of a functional synapse. The *left panel* shows a PV-positive interneuron soma (*red*; appears flat because it was on the cutting plane of the section) in somatosensory area SIV. However, around the perimeter of this interneuron two contacts from auditory FAES axons (*green*) and numerous vGlut1-positive (*blue*) points are visible. The *right panel* shows a digital enlargement of the boxed FAES bouton (*green*)–SIV interneuron (*red*) anatomical contact. The *white arrows* indicate the precise position of vGlut1-immunoreactive points that are visible when the FAES axon is rendered transparent, as depicted in the *lower right panel* (vGlut1-positive points are *blue* at *arrow tips*). The presence of vGlut1 at this axon-interneuron contact is indicative of a functional, glutamatergic synapse. Average voxel dimension ~200 nm, *scale bars* 1 μm

Table 1

Cross-modal anatomical contacts on SIV interneurons by calcium-binding class

	# (% of class)			Total
	CR+	CB+	PV+	
All neurons	196	60	27	283
Neurons w/contacts	76 (39)	24 (40)	12 (44)	112 (40)
1 contact	46 (60)	11 (46)	7 (58)	64 (57)
>1 contact	30 (40)	13 (54)	5 (42)	48 (43)
Soma only	34 (45)	11 (46)	8 (66)	53 (47)
Dendrite only	30 (40)	7 (29)	3 (25)	40 (36)
Soma + dendrite	12 (15)	6 (25)	1 (9)	19 (17)

The different types of somatosensory SIV interneurons, as labeled by calcium binding proteins (*CR* Calretinin, *CB* Calbindin, *PV* Parvalbumin) shows similar affinities for anatomical contacts based on type, number and location, by cross-modal inputs from auditory FAES